The Drosophila ovarian terminal filament imports molecules needed for lipid droplets, the fusome, and functional germ cells

Bhawana Maurya and Allan C Spradling

[1]Howard Hughes Medical Institute Research Laboratory

Carnegie Institution for Science

3420 San Martin Dr., Baltimore, MD 21212

ABSTRACT

Insect ovarioles begin with a protruding stack of flat cells known as the terminal filament (TF) located in species such as Drosophila just upstream from germline stem cells (GSCs) in the germarium. Terminal filaments function during development, but an adult role has not been clearly established. TF-specific disruption of exocyst vesicle trafficking genes indicated that each TF stack continuously imports at least $0.75\mu^3$ of lipophilic molecules per day, and transfers them through the cellular stack into the GSC region. When lipid import between the TF and germ cells is cut off, LDs accumulate in TF cells, stem cell function and spectrosome size decreases, cyst formation and fusome structure is altered and follicle development becomes abnormal. Knockdown of organic anion transporter Oatp30B in the TF blocked the differentiation of GSC daughters, generating a tumor. The Oatp30B human ortholog SLCO5A1 has prognostic value in ovarian cancer. In sum, the terminal filament is essential to import ovarian lipids required for normal germ cell development and oocyte production.

INTRODUCTION

Ovaries in most insect species are divided into ovarioles containing germline cysts and ovarian follicles lined up in developmental order, like an assembly line (reviewed in Büning, 1994). Characteristically, each ovariole starts with a "terminal filament (TF)," described in the earliest study of an insect ovary by Malphigi in 1669 (see Gall, 1996) but whose functional significance in egg production has remained unclear (Figure 1A). TF cells are flattened like a stack of coins, and vary greatly in number between species (Büning, 1994; Sarikaya et al. 2011). TFs were proposed in the past to act as a "ligament" to mechanically anchor the ovary to the abdominal wall. However, they lie inside the outermost ovarian tissue, the ovarian sheath, which loosely bundles all the ovarioles.

Terminal filaments are important during ovariole differentiation and constitute the first recognized ovariole structure in the third instar larval ovary. Precursor cells anterior to the germ cells migrate and intercalate in a spatially and temporally graded fashion along the medial-lateral axis to gradually form 15-20 TF stacks (King, 1970; Godt and Laski, 1995; Sahut-Barnola et al. 1995). TF precursors begin to express two similar and essential BTB domain transcription factors *bric-a-brac 1* and *2 (bab1 and bab2)* prior to stack formation (Godt and Laski, 1995). L3 larval TF cells also turn on the signaling molecule *hedgehog (hh)* (Forbes et al. 1996). Drosophila terminal filament structure changes more rapidly than other anterior ovariolar features during adulthood but reasons remain unknown (Forbes et al. 1996).

Terminal filaments promote germline stem cell (GSCs) niche development in early pupal ovaries. TF cells use Notch signaling to specify a new cell type, cap cells, that connect with both the basal TF and directly bind GSCs. Every 2-3 cap cells induced allows the niche to support one more GSC (Song et al. 2007). After niche completion, a continuing role for the TF is less clear.

In Drosophila, over the first two weeks post eclosion, basal TF cells remain associated with the cap cells and maintain hh expression, but a gap sometimes forms between them and more anterior TF cells that shut off hh. Some insects that produce many offspring, like honeybee (*A. mellifera)* queens, contain TFs with 10 times more flat TF cells than are found in the Drosophila TF. Queens produce about twice as many eggs per ovariole per day over a lifespan that is 15-20 times longer than Drosophila females (Cullen et al 2024), suggesting the TF contributes to ovariole activity or longevity. Honeybee terminal filaments preside over an expanded niche housing about 20 8-cell, fusome-containing germline cysts that function as GSCs. These GSC-like cysts do not decline in number with age, but TF action seems to work at a distance because they only divide in the middle of the GSC region (Cullen et al 2024).

The well-studied Drosophila TF contains 8-9 flattened somatic cells that protrude from the end of each ovariole anteriorly, while the posterior ends contact niche cap cells (Figure 1A). With 5 or more cap cells (Figure 1A, yellow) and at least 4 special escort cells (Figure 1A, blue) GSC niches typically house and adhere strongly with two GSCs. Each GSC contains a large spherical spectrosome located near the site of cap cell contact that develops into the fusome of developing germline cysts (Figure 1B; deCuevas and Spradling, 1998).

The niche constitutes a signaling hub that maintains GSC identity by secreting Bone Morphogenetic Protein (BMP) ligands including Decapentaplegic (Dpp) that locally inhibit GSC differentiation. Daughter "cystoblasts" begin developing as they as they exit the niche and produce 16-cell cysts. Cysts interact with additional stable squamous escort cells until about halfway through the germarium when they acquire epithelial stem cell (FSC)-derived follicle cells (Figure 1A, green) that grow to encase them in a monolayer shortly before they bud from the germarium as a new follicle (Hinnant et al. 2020). During cyst development, the spectrosome

develops into the fusome, a structure that contains most germ cell endoplasmic reticulum (ER) and branches between all the cells by passing through ring canals. The fusome is labeled by antibodies to several protein isoforms of the the *hu-li tai shao (hts)* gene (Petrella et al, 2007). GSCs and forming cysts greatly expand the amount of fusome they contain during their residence in the germarium but sources of fusome material other than internal biosynthesis have not been identified.

We carried out genetic knockdown experiments (using bab1-GAL4) both throughout development and in adulthood (using also GAL80^{ts}). We found that adult terminal filaments serve continuously as a source of molecules, especially lipids, using precursors that are likely taken up from the hemolymph, including by the LpR2 and the Oatp30B receptors. TF-dependent vesicle trafficking and transporter activity are essential for the normal production of germ cell lipid droplets, fusomes, and for cyst development. The expression and requirement for the Oatp30B transporter in TF cells suggests that that a novel steroid substrate is imported by the TF and functions in ovary regulation.

RESULTS

Early germ cells contain lipid droplets and fusomes

We looked for cellular components within germ cells near the TF that might be supported by its activities. Lipid droplets (LDs), including some of substantial size, were stained in each early germ cell using BODIPY 493 or Nile red (Figure1B-C). They were also labeled with LipidTox, neutral lipid dyes that specifically mark lipids stored within LDs (Figure 1D). Germ cells contained the most LDs, and these LDs preferentially stained with Bodipy (Figure 1E). In contrast, very few LDs were detected in TF cells, and these appeared as tiny, easily overlooked structures with any of the dyes (Figure 1F-H, E, J, S 1E). Since germ cells and follicle cells are

constantly being produced and moving posteriorly in the ovariole, the source of their LDs was unclear.

A similar mystery applies to the germ cell fusomes. Small TF-resident Hts-positive structures (Figure 1F, triangle), from 0.2 to 1.2 µm in size (Figure S1 F), much smaller than spectrosomes and fusomes were detected. However, Hts-positive vesicles in TF cells were only present during day 1-2 following eclosion (Figure 1F-I). This restricted time frame suggested they might represent delayed adult tissue completion, or a product derived from larval fat body cells, which is present in the adult abdominal cavity only during the first two days of adulthood.

Terminal filament cells transport lipids to germ cells via exocyst-dependent vesicle trafficking

If TF cells exchange lipids with cap cells that ultimately appear in germ cells, the exocyst would almost certainly be required (Meek et al. 2024). The exocyst complex represents a key effector of polarized exocytosis, and is responsible for tethering secretory vesicles to specific plasma membrane domains prior to fusion. Although the exocyst is used by most or all cells, and is critical for cytokinesis in mitotically cycling cells, adult TF cells do not cycle or divide and appear fully differentiated. Sec6 is a key exocyst component due to its binding to Rab9 at the plasma membrane and to Rtnl1 in the ER (Morgera et al. 2012). In an initial experiment, knocking down Sec6 using a *bab1-Gal4* driver (Figure S1A) caused a severe depletion of mature oocytes in the ovary and daily egg production never exceeded low levels (Figure 2A-C). We confirmed that the TF has active exocytosis using FM1-43 dye, which labels vesicles undergoing membrane recycling and regulated exocytosis (Figure S1B). FM1-43 is widely used in studies of synaptic activity and neurogenesis, where it marks vesicle turnover during neurotransmitter release. *Sec6* knockdown significantly reduced FM1-43 signal in TF cells (Figure S1C, D).

To provide further insight, we limited the knockdown not only to bab1-expressing cells, but also to adulthood using *bab1-GAL4, tub-Gal80^{ts}*. Females were initially maintained at 18 °C to allow Gal80^{ts} mediated repression of Gal4 activity, then shifted to 29 °C to inactivate Gal80^{ts} and induce RNAi knockdown after ovarian development was complete in late pupae. Under these conditions, *Sec6* knockdown in TFs led to a marked reduction in LD levels throughout the germarium, as revealed by BODIPY 493/503 staining (Figure 2D–F). Interestingly, while LDs were depleted from germ cells, large LDs accumulated specifically in posterior TF and cap cells in *Sec6* knockdown animals compared to control (Figure 2 G-H). Quantitative analysis confirmed a significant increase in LD size and number in the TF region (Fig2 I). This phenotype suggests that under normal conditions, the TF lipids imported or produced by TF cells move through quickly in small vesicles, rendering them difficult to see. However when exocytosis is disrupted, vesicle movement is slowed or blocked, and they back up, accumulate and fuse into larger particles in the TF and cap cells. These findings highlight a previously unrecognized function of the TF in lipid transport into germline and somatic cells that supports follicle development.

<u>Knockdown of multiple exocyst components affect lipid vesicle trafficking:</u>

Using the same protocol, knockdown of other exocyst components (*Sec10*, *Sec15*, *Sec5*, *Exo70*, *Exo84*) also resulted in LD depletion in the germarium (Fig 2J-O, P), although *Sec6* knockdown produced the most severe phenotype, with near-complete LD loss. It was surprising that the weaker knockdowns showed much less backup of LDs in the TF, yet they still strongly impaired the accumulation of LDs throughout the germarium after several days. This suggested that developing ovarian cells preferentially utilize most available lipids when they are limited,

and that lipid mobility within the germarium is more rapid than the slow movement of germ cells themselves.

Stem cell function and cyst production depend on a continuous flow of materials from the TF

To examine in more detail how disrupted trafficking from the terminal filament affects ovarian development, we again performed *Sec6* knockdown in TF cells using *bab1-GAL4*, *tub-GAL80*^{ts} flies. Flies were shifted to 29 °C at the late pupal stage, long after TF morphogenesis is complete and ovaries analyzed every two days post-eclosion (Figure 3A-E). Controls lacking *sec6* RNAi were treated identically (Figure 3A). These experiments revealed several new insights. First, LDs rapidly backup in the TF, since the number of accumulated vesicles had already increased greatly after just 2 days and did not rise significantly thereafter (Figure 3 A-E, F). Similarly, the number of LDs in the germarium as a whole dropped precipitously by 2 days, and remained at this level at later times (Figure 3 A-E, G). However, the total volume of Bodipy-stained lipid in the TF increased steadily at least until 8 days post eclosion, but was stored through increases in droplet volume (Figure 2H). In contrast, LD levels in the germarium remained at the same low level throughout all observed time points (Figure 3A–G,H). This argues that exocyst function is needed for lipids taken up in TF cells to exit from cap cells into ovariolar germ and somatic cells.

The results for Hts aggregates were slightly different (Figure 3A'-E', J). A substantial initial TF accumulation was observed at 2 days, but it did not grow further. This suggests that Hts aggregates, like lipid droplets, become trapped in the TF in the absence of exocyst activity, but since their import or production ceases normally after 2d (Figure 1I) no further TF buildup is seen.

A second major conclusion was that losing cargo import from TF into the ovariole rapidly affected stem cell and cyst behavior. 2 days after temperature shift, the germarium retained relatively normal structure (Figure 3B vs 3A), but GSC spectrosomes were smaller and already fragmented (Figure 3B' vs 3A'; Figure 3K). At 4 days, in addition to spectrosome defects, cyst development was deranged, as region 2a contained many more cysts, but they were smaller and incompletely developed (Figure 3C vs 3A). At 6 days and 8 days, cyst development had dropped further and germaria were half their normal size with multiple defects (Figure 3D, 3E vs 3A and 3B).

We knocked down Sec6 in escort cells to investigate whether these cells contribute to lipid import into germ cells. We used *c587-GAL4* which strongly labels escort cells but also FSCs and early follicle cells. Despite its function throughout development, no buildup of LDs in the TF or in other cells was observed, and the levels of LDs in the germarium were similar to controls (Figure 3 L, M). A small disruption of development may have occurred, but far less than the disruptions caused by loss of terminal filament input just in adult ovaries using GAL80^{ts}. Unlike TF knockdown of sec6, LD levels in germ cells following c587-driven KD were not significantly reduced (Figure 3N). We conclude that escort cells do not make a substantial contribution to the supply of germ cell lipids and fusome materials. Rather, the TF and cap cells appear to be the main lipid-donating somatic cells in the germarium.

<u>Terminal filament express transporters that influence germ cell development</u>

Considering the important role of cargo uptake from the hemolymph into the TF revealed by these experiments, we searched for candidate transporters expressed in these cells (Slaidina et al., 2021). We initially examined LpR2, a lipophorin receptor known to mediate uptake of

neutral lipids from the hemolymph (Matsuo et al., 2019) and to function in lipid yolk accumulation in later follicles (Sieber and Spradling, 2015).

We performed TF-specific knockdown of LpR2 as previously using *bab1-GAL4* and *GAL80ts*. Following knockdown, we observed a reduction in lipid accumulation throughout the germarium, and defective cyst formation, indicating that LpR2-mediated lipid uptake by TF cells is critical for maintaining lipid levels in this tissue (Figure 4 A,B, E). We also examined Oatp30B, whose selective expression in the TF was discovered by enhancer trap screening (Figure 4D). We knocked down Oatp30B in TF cells as before. Disruption of Oatp30B function in TF cells caused a marked reduction in lipid droplet levels within the germarium (Figure 4 A, C, E), indicating that *Oatp30B* contributes to lipid delivery or uptake in developing germ cells. In addition to lipid reduction, Oatp30B knockdown also resulted in differentiation defects in the germline. Normally, spectrosomes are restricted to germline stem cells and their daughter cystoblasts (CBs). The anterior germarium contains about 3 spectrosome-containing cells (Figure 4A), however, after shifting bab1-GAL4. GAL80ts ; UAS-Oatp30B_RNAi flies to the restrictive temperature for 3 days caused an accumulation of 7-8 cells containing spectrosomes per germarium, largely filling the space up to region 2A (Figure 4C, F). This shows that GSC activity continued but germ cell development beyond the GSC was arrested.

Oatp30B is a candidate transporter for the cardiac glycoside ouabain, which acts by inhibiting the Na□/K□-ATPase and locking it in a non-functional conformation. Evidence for production of an endogenous source of a ouabain-like molecule has been obtained in both mammals (Laredo et al. 1995; Hamlyn JM et al. 1991) and insects (Torrie et al. 2004) but a biosynthetic pathway has remained unclear. The Drosophila Na/K-ATPase alpha subunit contains a highly conserved ouabain binding site (Dostanic-Larson et al. 2005). Furthermore,

immunostaining revealed that its target, Na□/K□-ATPase, is highly enriched in TF cells (Figure 4 G, H). Strikingly, TF-specific knockdown of *Oatp30B* significantly reduced Na□/K□-ATPase expression (Figure 4 I, J) suggesting that the uptake of small organic molecules via Oatp30B may regulate ion pump expression or stability in niche cells.

To investigate the downstream consequences of ion imbalance, we examined the status of Hedgehog (Hh) signaling, which is known to be regulated by membrane potential and ion flux in other tissues such as the wing disc (Emmons-Bell et al., 2021). Hh signaling plays a critical role in TF organization and stem cell niche maintenance. In controls, Hh expression was detected in TFs; however, in Oatp30B knockdown ovaries, Hh expression was markedly reduced (Figure 4K-L, M), indicating that disruption of Oatp30B and its downstream ionic balance may impair Hh-mediated niche signaling.

Lipid droplets in the germarium protect against mitochondrial ROS accumulation:

Why does the germarium require a continuous supply of lipids, and do LDs serve functions beyond energy storage? We have observed that LDs in early germ cells are frequently in close proximity to mitochondria in the germarium (Figure 5A). This spatial association is consistent with earlier reports suggesting that LD–mitochondria contacts facilitate fatty acid transfer**,** enabling mitochondrial respiration and regulating oxidative homeostasis (Nguyen et al., 2017; Rambold et al., 2015). Disruption of these contacts or LD content has been linked to elevated mitochondrial reactive oxygen species (ROS) and organelle dysfunction.

To directly test whether **l**oss of lipid droplets leads to ROS accumulation**,** we knocked down the lipogenic gene Acetyl-CoA Carboxylase (ACC) in germ cells using *nanos-GAL4.* ACC is a key enzyme in de novo fatty acid synthesis and is essential for neutral lipid production. ACC knockdown resulted in a dramatic reduction or complete loss of LDs throughout the germarium

(Figure 5B–D). We next assessed mitochondrial ROS using MitoSOX and DHE staining. Both assays showed significantly elevated ROS levels in ACC-depleted germarium compared to controls (Figure 5E–F, H-I, K, L), indicating oxidative stress resulting from lipid depletion.

To determine whether this ROS phenotype also arises when LD transport from the TF is impaired, we examined TF-specific knockdown of *Sec6*. As previously shown, *Sec6* knockdown blocks vesicular transport of lipids to the germarium. Consistent with our hypothesis, *Sec6*-RNAi in TFs also led to elevated mitochondrial ROS in germ cells, as measured by both MitoSOX and DHE (Figure 5E–G, H, J K, L).

DISCUSSION

The terminal filament imports molecules from the hemolymph and transfers them into the ovariole to support GSCs and oocyte production

Our experiments demonstrate that a major adult function of the Drosophila terminal filament is to important lipids and other molecules into the GSC region to support stem cell divisions, germ cell cyst formation and follicle development. Knocking down the exocyst subunit Sec6 in the TF blocked the ability of lipid droplets to be transferred from TF cells to cap cells and into the anterior germarium germ cells causing LDs to build up in the TF. Blocking TF import had immediate deleterious effects on GSCs and their daughter cystoblasts, whose spectrosomes became altered in structure, and which failed to developed normally.

When cargo import from the TF is shut off, germarium lipids drop to a much lower level that likely reflects an equilibrium based on residual entry and endogenous synthesis that dictate lower use levels. We estimate from the kinects of LD building that the TF takes up/synthesizes at

least $0.75\mu^3$ per day of Bodipy-stainable lipid. This dye is thought to specifically reveal core lipids within LDs, so additional cargo reductions may also occur.

Fluctuating nutrient supplies are a common condition during reproduction, but these changes do not usually exert effects such as observed following transport cutoff from the TF. When food resources become limited follicle production rapidly slows down, but continues to produce normal follicles, with little change in ovariole appearance. Checkpoints ensure that that the cyst and follicle numbers and distribution remain normal, except at a few specific transition points, such as the onset of vitellogenesis at stage 8. TF import, in contrast, is essential for ovarioles to function normally even for a short period and to prevent the rapid production of abnormal intermediates. Probably, many molecular species are produced from dietary inputs, that are processed and stored in the fat body, as occurs in mammalian liver and fat tissue. Stored resources can be released as needed over many days to maintain production of fully functional oocytes at a lower level. However, without a functioning terminal filament, critical regulators or materials run short almost immediately. Normally, the TF may always remain able to import enough of these critical regulators that it is unnecessary to store them locally in the ovary.

<u>The terminal filament also transports vesicles rich in Hts protein during the first 2 days of adult life.</u>

We documented that movement of Hts-containing vesicles in the terminal filament of newly eclosed adults ceases after two days. In contrast to LDs, the natural cessation of Hts vesicle production caused these particles to plateau in the TF when transport into the ovariole was blocked. Most likely, these are contributed by the larval fat body cells that remain in the abdomen during the first 1-2 days, and are thought to provide nutrients as the adult gut completes its development and becomes active (Obniski et al. 2018). Our experiments could not distinguish

where TF molecules in the LDs or in the Hts particles are responsible for the phenotypes following import failure.

Oatp30B transports a critical molecule for cyst production

It was surprising that the effects of knocking down Oatp30B on cyst development were stronger than the effects of completely blocking TF import using sec6 RNAi. This observation suggest that there may be a major regulator of stem cell differentiation that acts by undergoing import into ovarioles via the TF. Such a molecule would have to be unable to enter the germarium via direct import through other somatic cells, but be able to bypass the block in exocyst function in the TF, suggesting there may be another pathway from TF to ovariole that does not require vesicle trafficking.

Import via the terminal filament may be essential to high quality components

The strong dependence of ovarian lipid droplets in the early ovary on particular source may arise simply because there are few alternatives to the terminal filament for lipid acquisition in the ovariole anterior. However, there is a high flux of precursor molecules overall from the gut to the ovary under favorable environmental conditions. Drosophila females are able to lay a substantial fraction of their weight in eggs each day, a prodigious feat suggesting that internal ovarian transport is not likely to be rate limiting. More likely to be challenging than simple transport in producing gametes is the need for lipid quality imposed by germ cell rejuvenation, the elimination of modified lipids that catalyze errors that might begin to increase in subsequent generations. TF-derived lipids may be relied upon for example, because movement through the TF may involve a process of quality selection.

Lipids absorbed in the diet are typically distributed through the hemolymph as lipoprotein particles for uptake by cells for their use. Our findings suggest that early germ cells, which do not have direct access to the hemolymph but have a strong need for lipids for growth, do not simply take up lipids from the hemolymph on a cell autonomous basis like in many somatic tissues. The terminal filament appears to take up dietary lipids directly from hemolymph, and transfer them to germ cap cells and then to germ cells and possibly to niche cells somatic cells. When we strongly disrupted sec6 in the TF, a significant buildup of lipids occurred in multiple TF cells. This shows that multiple cells take up LDL particles and transport them from cell to cell by endocytic trafficking, exocytosis, within multiple TF cells and then cap cells. At this point, transported products contact and may enter into a GSC, cap cell, or into an escort cell, that contacts cap cells.

There are thousands of lipid species and many ways that they can become modified with innumerable possible adducts. To generate fresh membranes without a history of past modifications, germ cells may strive to resynthesize as many molecules as possible over in germ cells. This could lead them to use the TF to take up precursors and purify away all lipid contaminants as they move along the TF stack. Thus, the TF may function like a lipid column, purifying the incoming fatty acids, TGs etc. with the end result of supplying the GSC niche with the best possible materials for generating new plasma and organelle membranes.

TF-like interfollicular "stalk" cells may provide a similar function to follicles

Our findings also suggest a reason that follicles in ovarioles are connected by interfollicular stalks. Some of the most critical oocyte components such as organelles may be rebuilt in the germarium during the meiotic stages associated with rejuvenation in lower

eukaryotes. Although the very best membranes might already have been used to reconstitute the organelles of the Balbiani body, additional organelles and membrane lipids are still needed in cytoplasm that will be used in somatic cells. The great majority of growth based on volume increase takes place after the first follicle has formed. Consequently, several additional cell types with terminal filament,-like architecture, namely interfollicular stalk cells, may serve a related function as a source of input and quality control for the uptake of hemolymph lipoproteins. These smaller "filters" may still provide value in removing the alterations that are likely to be found in dietary lipids taken up directly from the gut or fat body. Finally, the terminal web of the pupal ovary has one the longest sequence of TF-like cells, and it may provide nutrients at a critical time as the first follicles to derive from stem cells begin to appear.

The terminal filaments may regulate activity levels ovariole by ovariole

There is a large variation in the number of ovarioles, and TF cells per ovariole across diverse Drosophila species and among other insects (Sarikaya et al. 2011). However, there has been little progress in understanding their biological and functional significance due to limited understanding of TF physiology and until recently, TF gene expression. Our results suggest that the terminal filament plays a major role in controlling the overall rate of function of the ovary via its control of import of lipid precursors for membrane production, secretion and hormone import and storage. Positioned at the head of the ovariole, the TF is well located to regulate its associated ovariole autonomously. Major effectors of this control are likely steroid hormones (Morris and Spradling, 2011). The follicle cells produce and secrete ecdysone locally in follicles to coordinate cellular behavior that allows stage-specific development. Some estrogen likely is secreted into the hemolymph as the circulating level of estrogen is substantially higher in females than in males. This secretion is thought depend on insulin gut enteroendocrine peptides to ensure

that the level of overall egg production matches the available resources. The terminal filament likely responds to these signals due to its proximity to the GSC niches, and ensures that GSC division and follicle production is maintained in all ovarioles.

Relatively little is known about how follicle development is coordinated to keep the same number and approximate stage distribution matched across 32 ovarioles spread across two ovaries. The terminal filament assisted by stalk cells and calyx cells at the base of the ovary, may help support and coordinate these processes. All the stem cells and downstream cells are used at similar levels initially, but if one suffers delays or becomes stalled the activity of the others adjusts to maintain the output of the organ as a whole. This regulation continues up to ovulation, where there is efficient, equal usage of individual ovarioles using regulatory paradigms that have been conserved to mammals (Knapp and Sun, 2017; review; Berg et al. 2024).

Ovariole regulation by TFs may utilize a novel steroid regulator sensed by Oatp30B

The terminal filament may act by controlling the importation of regulatory steroid hormones. During pupal development, the TF highly expresses a different Oatp gene, Oatp74D, which has been shown to be capable of transporting ecdysone (Scanlan et al. 2023). In adults the TF highly expresses Oatp30B, which is closely related to the human importer SLC05A (Roshandel et al. 2023). In humans, SLC05A1 is thought to transport estrogen derivatives. Its prognostic value for better ovarian cancer outcomes may result from a role supporting continuing estrogen dependence of these tumors (Svoboda et al. 2018). A genetically tractable model of Oatp30B function in the ovary would be valuable for identifying regulators of mammalian and insect ovaries that remain little characterized, such as endogenous ouabain.

LDs may not serve merely as lipid storage depots but may function to maintain redox balance in early germ cells. LDs may buffer excess free fatty acids, distribute lipids to

mitochondria in a regulated manner, and prevent lipotoxic stress. In the absence of LDs, free fatty acids can undergo peroxidation**,** triggering a cascade of oxidative damage (Listenberger et al., 2003; Bailey et al., 2015). LDs are also important in the nervous system to protect against the deleterious effects of lipid peroxidation by transporting them to glial cells for removal (Moulton et al. 2021). Maintenance of this capacity could also contribute to cancer resistance.

METHODS

Fly Genetics

All *Drosophila melanogaster* stocks were maintained on standard cornmeal agar media at room temperature unless otherwise specified. The Oregon R strain was used as the wild-type control throughout the study. The GAL4 driver lines *bab1-GAL4*, *c587-GAL4*, and *nanos-GAL4* were obtained from the Bloomington Drosophila Stock Center (BDSC). UAS-RNAi lines were obtained from the Vienna Drosophila Resource Center (VDRC), including *Sec6-RNAi* (VDRC #22077), *Sec15-RNAi* (VDRC #35161), *Sec10-RNAi* (VDRC #318483), *Sec5-RNAi* (VDRC #28873), *Exo70-RNAi* (VDRC #103717), *Exo84-RNAi* (VDRC #108650), *Oatp30B-RNAi* (VDRC #110237), LpR2 (VDRC #25684) and *ACC-RNAi* (VDRC #8105). All genetic crosses were performed at 25 °C unless otherwise noted. For temporally controlled gene knockdown, the temperature-sensitive Gal80 system (*tub-GAL80^{ts}*) was used in combination with *bab1-GAL4*. Crosses were maintained at 18 °C to allow GAL80^{ts} mediated repression of GAL4 activity during development. Adult progeny was then shifted to 29 °C to inactivate GAL80^{ts} and permit GAL4 driven RNAi expression at desired developmental stages.

Egg Laying Assay

Newly eclosed (0–1 day old) flies were maintained in plastic bottles containing molasses plates overlaid with a layer of wet yeast, replaced daily. For egg laying measurements, five pairs of flies were kept per bottle, and the number of eggs laid was counted every 24 hours, in triplicate.

Immunostaining:

Immunostaining was performed on ovaries dissected from adult *Drosophila melanogaster* females. Dissections were carried out in Grace's insect medium, followed by fixation in 4% paraformaldehyde (PFA) with 0.01% PBST (PBS with 0.01% Triton X-100) for 30 minutes at room temperature. Fixed ovaries were then blocked in 5% Normal Goat Serum (NGS) for 1 hour and incubated overnight at 4°C with primary antibodies diluted in blocking solution. After extensive washing with PBST, samples were incubated with secondary antibodies (1:200 dilution) for 2 hours at room temperature. DNA was counterstained with DAPI (0.5 µg/mL), and samples were mounted in Vectashield mounting medium. Confocal images were acquired using a Leica STELLARIS 8 DIVE microscope. Intensity profile graphs were generated using Image J (NIH) and GraphPad Prism software.

The following primary antibodies were used: mouse anti-Hts (1:100; DSHB), chicken anti-α5 (1:200; DSHB), mouse anti-LaminC (1:50; DSHB), rabbit anti-Cytochrome C (1:50; Cell Signaling Technology), and rabbit anti-Hedgehog (1:500; kindly provided by Dr. Tom Kornberg).

Nile Red, BODIPY 493/503 and LipidTOX™ Deep Red Staining

To visualize neutral lipids, tissues were dissected in 1× PBS and fixed in 4% paraformaldehyde for 20 minutes at room temperature. Samples were washed three times with 1× PBS and incubated in Nile Red solution (1 µg/mL in PBS), LipidTOX™ Deep Red (1:500), BODIPY 493/503 (1 µg/mL in PBS) for 30 to 45 minutes in the dark. After staining, tissues were washed

briefly with PBS, counterstained with DAPI (0.5 µg/mL), and mounted in Vectashield for imaging. Images were acquired using a confocal microscope.

FM1-43 staining

Ovaries were dissected in ice-cold 1× PBS and incubated in FM1-43FX dye (5 µg/mL in PBS; Thermo Fisher) for 15–20 minutes at room temperature in the dark. After staining, tissues were washed briefly with PBS and fixed in 4% paraformaldehyde for 20 minutes. Following fixation, samples were washed three times with PBS and mounted in Vectashield for imaging.

DHE and MitoSox Staining

To assess reactive oxygen species (ROS) levels, freshly dissected ovaries were incubated in Schneider's Drosophila medium containing either dihydroethidium (DHE; 5µM, Invitrogen) or MitoSOX™ Red (5 µM, Invitrogen) for 10–15 minutes at room temperature in the dark. After staining, tissues were washed twice with 1× PBS and fixed in 4% paraformaldehyde for 20 minutes. Samples were then rinsed, mounted in Vectashield with DAPI, and imaged using a confocal microscope.

Statistical Analysis:

All experiments were performed in triplicate. Data were analyzed using GraphPad Prism version 10 and are presented as mean ± standard deviation (SD). Statistical significance was assessed using one-way ANOVA, with $p < 0.05$ considered significant.

ACKNOWLEDGEMENTS

We thank Mahmud Siddiqi for assistance with light microscopy and Mike Sepanski for electron microscopy. Dianne Williams assisted with Drosophila stock management. We are

grateful to Asya Davidian, Haolong Zhu, Madulika Pathak, Ashish Tiwari, Yunpeng Fu, Andy Mao and other members of the Spradling laboratory for discussions. Allan Spradling is an Investigator of the Howard Hughes Medical Institute, and HHMI provided support for these studies. The Carnegie Institution for Science has generously supported the Spradling lab in Baltimore for many years, for which we are grateful.

REFERENCES

Bailey, A. P., Koster, G., Guillermier, C., Hirst E.M.A., MacRae J. I., Lechene. C.P., Postle A.D., Alex P. Gould1. (2015). Antioxidant role for lipid droplets in a stem cell niche of *Drosophila*. *Cell*, **163**(2), 340–353.

Berg C, Sieber M, Sun J. (2024). Finishing the egg. Genetics. 226: iyad183. doi: 10.1093/genetics/iyad183.

Büning J. (1994). The Insect Ovary: Ultrastructure, Previtellogenic Growth and Evolution.Chapman and Hall. DOI:https://doi.org/10.1007/978-94-011-0741-9.

Cullen G, Delargy E, Dearden PK. (2024). Development of germline progenitors in larval queen honeybee ovaries. Biol Open. 13, bio060511. doi: 10.1242/bio.060511.

de Cuevas M, Spradling AC (1998) Morphogenesis of the Drosophila fusome and its implications for oocyte specification. Development 125:2781–2789. https://doi.org/10.1242/dev.125.15.2781

Dostanic-Larson I, Van Huysse JW, Lorenz JN, Lingrel JB. (2005). The highly conserved cardiac glycoside binding site of Na,K-ATPase plays a role in blood pressure regulation. Proc Natl Acad Sci U S A. 2005 Nov 1;102(44):15845-50. doi: 10.1073/pnas.0507358102.

Forbes, Z., Lin, H., Ingham, P. and Spradling, A.C. (1996). *hedgehog* is required for the proliferation and specification of somatic cells prior to egg chamber formation in Drosophila. Development 122: 1125-1135.

Gall JG. (1996). Views of the the Cell: a pictorial history. American Society for Cell Biology Press.

Godt D, Laski FA. (1995). Mechanisms of cell rearrangement and cell recruitment in Drosophila ovary morphogenesis and the requirement of bric à brac. Development. 121, 73-87. doi: 10.1242/dev.121.1.173.

Hinnant, T. D., Merkle, J. A., & Ables, E. T. (2020). Coordinating Proliferation, Polarity, and Cell Fate in the Drosophila Female Germline. Frontiers in Cell and Developmental Biology 8, 19. https://doi.org/10.3389/FCELL.2020.00019.

King RC. (1970). Ovarian development in Drosophila melanogaster. Academic Press.

Knapp E, Sun J. (2017). Steroid signaling in mature follicles is important for Drosophila ovulation. Proc. Natl. Acad. Sci. U.S A., 114, 699-704, 10.1073/pnas.1614383114.

Laredo, J., Hamilton, B. P., Hamlyn, J. M., et al. (1994). "Ouabain is secreted by bovine adrenocortical cells." *Endocrinology* 135(2):794-797–4881.

Listenberger, L. L., Han, X., Lewis, S. E., Cases, S., Farese, R. V., Ory, D. S., & Schaffer, J. E. (2003). Triglyceride accumulation protects against fatty acid-induced lipotoxicity. *Proceedings of the National Academy of Sciences, 100*(6), 3077–3082.

Matsuo, N., Nagao, K., Suito, T., Juni, N., Kato, U., Hara, Y., & Umeda, M. (2019). Different mechanisms for selective transport of fatty acids using a single class of lipoprotein in *Drosophila*. *Journal of Lipid Research*, *60*(7), 1199–1211.

Emmons-Bell M & Hariharan I K, (2021). Membrane potential regulates Hedgehog signalling in the *Drosophila* wing imaginal disc. EMBO Reports 22: e51861.

Hamlyn, J. M., Blaustein, M. P., Bova, S., DuCharme, D. W., Harris, D. W., Mandel, F., Mathews, W. R., & Ludens, J. H. (1991). Identification and characterization of a ouabain-like compound from human plasma. *Proceedings of the National Academy of Sciences of the United States of America*, *88*(14), 6259–6263.

Meek S, Hernandez AC, Oliva B, Gallego O. (2024). The exocyst in context. Biohemical Society Transactions 52, 2113-22.

Morgera F, Sallah MR, Dubuke ML, Gandhi P, Brewer DN, Carr CM, Munson M. (2012). Regulation of exocytosis by the exocyst subunit Sec6 and the SM protein Sec1. Mol Biol Cell. 23, 337-46. doi: 10.1091/mbc.E11-08-0670.

Moulton MJ, Barish S, Ralhan I, Chang J, Goodman LD, Harland JG, Marcogliese PC, Johansson JO, Ioannou MS, Bellen HJ. (2021). Neuronal ROS-induced glial lipid droplet formation is altered by loss of Alzheimer's disease-associated genes. Proc Natl Acad Sci U S A. 118, e2112095118. doi: 10.1073/pnas.2112095118.

Morris, L., and Spradling, A.C. (2011). Long-term live imaging provides new insight into stem cell regulation and germline-soma coordination in the Drosophila ovary. Development 138, 2207-2215.

Nguyen, T. B., Louie, S. M., Daniele, J. R., Tran, Q., Dillin, A., Zoncu, R., Nomura, D. K., & Olzmann, J. A. (2017). DGAT1-dependent lipid droplet biogenesis protects mitochondrial function during starvation-induced autophagy. *Developmental Cell*, *42*(1), 9–21.e5.

Obniski R, Sieber M, Spradling AC. (2018). Dietary Lipids Modulate Notch Signaling and Influence Adult Intestinal Development and Metabolism in Drosophila. Dev Cell. 2018 Oct 8;47(1):98-111.e5. doi: 10.1016/j.devcel.2018.08.013.

Petrella LN, Smith-Leiker T, Cooley L. (2007). The Ovhts polyprotein is cleaved to produce fusome and ring canal proteins required for Drosophila oogenesis. Development. 134, 703-12. doi: 10.1242/dev.02766.

Rambold, A. S., Cohen, S. L., & Lippincott-Schwartz, J. (2015). *Fatty acid trafficking in starved cells: Regulation by lipid droplet lipolysis, autophagy, and mitochondrial fusion dynamics.* Developmental Cell, 32(6), 678–692.

Roshandel D, Sanders EJ, Shakeshaft A, Panjwani N, Lin F, Collingwood A, Hall A, Keenan K, Deneubourg C, Mirabella F, Topp S, Zarubova J, Thomas RH, Talvik I, Syvertsen M, Striano P, Smith AB, Selmer KK, Rubboli G, Orsini A, Ng CC, Møller RS, Lim KS, Hamandi K, Greenberg DA, Gesche J, Gardella E, Fong CY, Beier CP, Andrade DM, Jungbluth H,

Richardson MP, Pastore A, Fanto M, Pal DK, Strug LJ; BIOJUME Consortium.(2023). SLCO5A1 and synaptic assembly genes contribute to impulsivity in juvenile myoclonic epilepsy. NPJ Genom Med. 2023 Sep 28;8(1):28. doi: 10.1038/s41525-023-00370-z.

Sahut-Barnola I, Godt D, Laski FA, Couderc JL. (1995). Drosophila ovary morphogenesis: analysis of terminal filament formation and identification of a gene required for this process. Dev Biol. 170, 127-35. doi: 10.1006/dbio.1995.1201.

Sarikaya DP, Belay AA, Ahuja A, Dorta A, Green DA 2nd, Extavour CG. (2012). The roles of cell size and cell number in determining ovariole number in Drosophila. Dev Biol. 363, 279-89. doi: 10.1016/j.ydbio.2011.12.017.

Scanlan JL, Robin C, Mirth CK. (2023) Rethinking the ecdysteroid source during Drosophila pupal-adult development. Insect Biochem Mol Biol. 152:103891. doi: 10.1016/ j.ibmb.2022.103891.

Sieber MH, Spradling AC. (2015). Steroid Signaling Establishes a Female Metabolic State and Regulates SREBP to Control Oocyte Lipid Accumulation. Curr Biol. 25, 993-1004. doi: 10.1016/j.cub.2015.02.019.

Slaidina M, Gupta S, Banisch TU, Lehmann R. A single-cell atlas reveals unanticipated cell type complexity in *Drosophila* ovaries. Genome Res. 2021 Oct;31(10):1938-1951. doi: 10.1101/gr.274340.120. Epub 2021 Aug 13. PMID: 34389661; PMCID: PMC8494228.

Song X, Call GB, Kirilly D, Xie T. (2007). Notch signaling controls germline stem cell niche formation in the Drosophila ovary. Development. 134, 1071-80. doi: 10.1242/dev.003392.

Svoboda M, Mungenast F, Gleiss A, Vergote I, Vanderstichele A, Sehouli J, Braicu E, Mahner S, Jäger W, Mechtcheriakova D, Cacsire-Tong D, Zeillinger R, Thalhammer T, Pils D.

(2018). Clinical Significance of Organic Anion Transporting Polypeptide Gene Expression in High-Grade Serous Ovarian Cancer. Front Pharmacol. 9, 842. doi: 10.3389/fphar.2018.00842.

Torrie, L.S., Radford, J.C., Southall, T.D., Kean, L., Dinsmore, A.J., Davies, S.A., Dow, J.A. (2004). Resolution of the insect ouabain paradox. Proc. Natl. Acad. Sci. U.S.A. 101(37): 13689-13693.

FIGURE LEGENDS

Figure 1: Localization of lipid droplets and Hts-positive aggregates in the terminal filament of the germarium.

(A) Schematic diagram of the germarium, highlighting the terminal filament (TF) at the anterior tip where germline stem cells (GSCs) reside. The position of follicle stem cells (FSCs) and the four recognized germarium subregions are shown. **(B-D)** Lipid Droplets (LDs) were observed throughout the germarium using BODIPY493/503, Nile Red, and LipidTOX staining. **(E)** Quantification of lipid droplet number in distinct cell types of the germarium. **(F-H)** LDs visualized using the neutral lipid dye BODIPY493/503 (arrow), and Hts immunostaining reveals Hts-positive aggregates (triangle) within TF cells 1, 3 or 8 days post-eclosion. **(I)** Decline and disappearance of Hts aggregates in the TF by day3 of adulthood. **(J)**. An EM showing a rare cross section through a cap cell and the thin cytoplasm of a posterior TF cell, reveals the presence of abundant small vesicles (arrow). bar: 2μ. SH sheath, EC escort cell, GSC germline stem cell.

Figure 2: Terminal filament delivers lipids to germ cells through exocyst-dependent vesicle trafficking.

(A) Wild-type germarium showing normal morphology. **(B)** Disrupted ovariole morphology upon TF-specific *Sec6* knockdown using *bab1-GAL4*. **(C)** Egg laying assay showing a significant reduction in the number of eggs produced per female per day following *Sec6* knockdown with *bab1-GAL4*. **(D)** BODIPY 493/503 staining of control germarium shows normal lipid droplet (LD) distribution at 8d post-ecolosion. (temperature shifted to 29 °C at late pupal stage). **(E)** Conditional knockdown of *Sec6* in terminal filament cells using the *bab1-GAL4, tub-Gal80^{ts}* shows substantial depletion of lipid droplets by day 8 post-eclosion. (temperature shifted to 29 °C at late pupal stage). **(F)** Quantification of LD number in control vs. *Sec6* knockdown, showing a significant decrease in LD number. **(G)** Control germarium showing normal LD levels in TF and cap cells at 8d post eclosion (at 29 ^{o}C). **(H)** Higher magnification of Sec6 KD in (E), showing accumulation of enlarged LDs in TF and cap cells, suggesting impaired lipid export due to disrupted exocytosis. **(I)** Quantitative analysis reveals a significant increase in LD number and size within the TF following *Sec6* knockdown. **(J-O)** Conditional knockdown of other exocyst genes at 8d post eclosion (temperature shifted to 29°C in late pupal stage). LaminC (TF marker), BODIPY (LDs), and DAPI (nuclei). **(J)** Control showing normal LDs distribution. **(K-O)** TF-specific knockdown of *Sec10, Sec15, Sec5, Exo70,* and *Exo84* results in LD depletion in the germarium **(P)**.

Figure 3: Terminal filament dependent transport of lipids and cytoskeletal component supports germ cell and cyst development.

(A) Control germarium showing normal distribution of lipid droplets (LDs) throughout the germarium. **(B–E)** LD staining (BODIPY 493/503) of germarium at days 2, 4, 6, and 8 post-eclosion following *Sec6* knockdown in terminal filament (TF) cells using *bab1-GAL4, tub-GAL80^{ts}*, with temperature shift to 29 °C at the late pupal stage. LDs accumulate within the TF, while their levels are markedly reduced in germ cells. **(B'–E')** Hts staining shows progressive accumulation of Hts-positive cytoskeletal aggregates in TF cells from day 2 to 8, these aggregates are absent in control germarium **(A')**. **(F)** Quantification of LD content in the TF following *Sec6* knockdown confirms significantly elevated lipid levels across time points.**(G)** LD quantification in the germarium shows consistent depletion following *Sec6* knockdown relative to controls. **(H)** Quantification of lipid volume in TF cells shows a steady increase from day2 to day8 in Sec6 knockdown compared with control. **(I-J)** Quantification shows increase in number and size of Hts aggregate per TF at days 2, 4, 6, and 8 post-eclosion in *Sec6* knockdown. **(K)** Quantification show that *Sec6*-depleted TF cells lead to reduced spectrosome volume in GSCs compared to control. **(L-M)** *Sec6* knockdown in escort cells driven by c587-GAL4 disrupts cyst and follicle formation, but LD levels in germ cells remain largely unaffected, compared to control (O). **(N)** Quantification of LD signal in germ cells shows no significant difference between control and escort cell specific *Sec6* knockdown, supporting a limited role for escort cells in lipid transport.

Figure 4: Oatp30B-mediated solute transport in the terminal filament regulates lipid delivery and germ cell differentiation.

(A) Control, LDs labeled with BODIPY 493/503 in A-C; **B)** Lipoprotein receptor LpR2 KD in the TF using *bab1-GAL4, tub-GAL80^{ts}* with RNAi induced at 29 °C in late pupal stage, and analyzed on day 7. LDs were reduced in the germarium **(E).** Organic anion transporter Oatp30B

is preferentially expressed in the TF **(D).** **(C)** Oatp30B KD in the TF was carried out as for LpR2. LDs were strongly reduced **(E).** Moreover, KD caused a block in cyst production indicated by a large increase in germ cells containing only a single spectrosome **(F)**. **(G)** Immunostaining with anti-Atpα reveals strong enrichment of Na□/K□-ATPase in terminal filament cells of control ovaries. **(H–I)** TF-specific knockdown of *Oatp30B* significantly reduces Na□/K□-ATPase levels, suggesting impaired regulation of ion pump expression or stability, as quantified in **(J).** **(K-l)** Hedgehog (Hh) staining shows robust expression in TFs of control ovaries (J), but is dramatically reduced upon *Oatp30B* knockdown **(L)**. **(M)** Quantification of Hh fluorescence intensity in the TF confirms a reduction following *Oatp30B* depletion.

Figure 5: Lipid droplets protect early germ cells from mitochondrial ROS accumulation. **(A)** Control germarium showing close association of lipid droplets (BODIPY 493/503) with mitochondria (Cyto C). **(B–C)** Control (B) and germ cell-specific *ACC* knockdown (C) ovaries (using *nanos-GAL4*), showing severe loss of LDs upon depletion of the lipogenic enzyme Acetyl-CoA Carboxylase. **(D)** Quantification of LD levels in germ cells shows a significant reduction following *ACC* knockdown. **(E–G)** MitoSOX staining reveals elevated mitochondrial ROS in *ACC* knockdown (F) and TF-specific Sec6 knockdown (G), compared to control (E). **(H-J)** DHE staining detects increased ROS levels in *ACC* knockdown (I) and TF-*Sec6* knockdown (J) germaria relative to control (H). **(K)** Quantification of MitoSOX signal intensity shows significant ROS increase in both *ACC*- and *Sec6*-depleted germaria. **(L)** Quantification of DHE signal intensity confirms significantly elevated ROS in both experimental conditions, supporting a protective role for LDs against oxidative stress.

Fig 6: Model for terminal filament uptake, intercellular transport and delivery of cargos to the ovariole.

Terminal filament (TF) cells actively incorporate molecules from the hemolymph, process and package them, and deliver resulting cargo including lipids, fusome components, and organic solutes to ovariolar germ cells and somatic cells via vesicle-mediated trafficking.

SUPPLEMENTALFIGURE LEGENDS

Fig S1: Active exocytosis in terminal filament with lipid droplet size and Hts-positive aggregate distribution.

(A) Ovariole tip from a bab1-GAL4; tub-GAL80ts>nlsGFP ovary stained with Lam-C, GFP and DAPI. The specificity of bab1 for the TF is evident. **(B-C-P)** FM1-43 dye staining in control germarium shows strong signal in TF and cap cells, indicative of active vesicle trafficking and membrane recycling. **(P)** FM1-43 staining is markedly reduced in TF and cap cells following *Sec6* knockdown, suggesting impaired exocytosis. **(D)** Quantitative analysis of FM1-43 fluorescence intensity confirms a significant reduction in TF/cap cells in *Sec6* knockdown samples compared to controls. (E) Number and size of LD within the TF, (F) Size of Hts aggregates ranging from 0.2 to 1.2 µm.

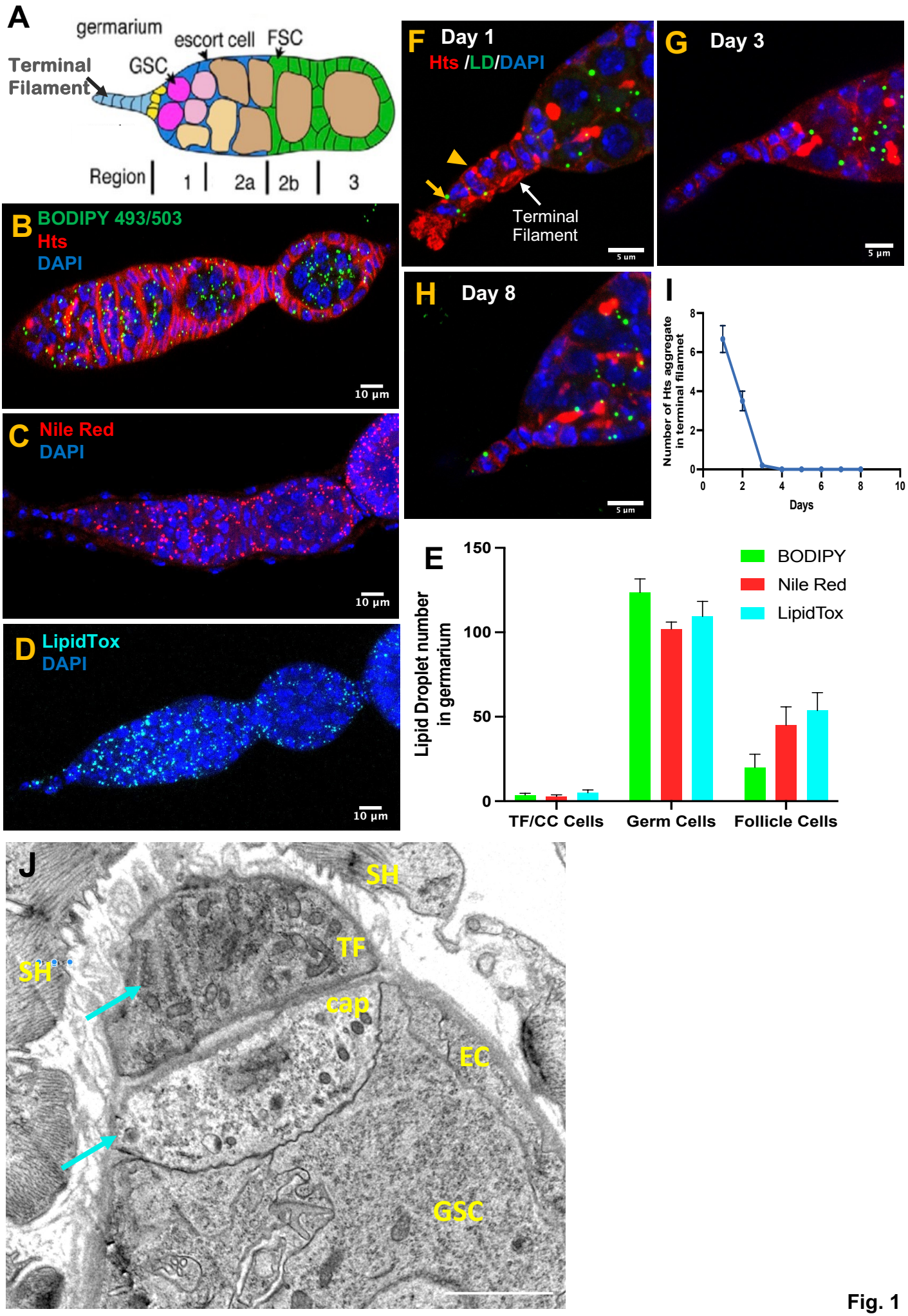
A
germarium
escort cell
FSC
Terminal Filament
GSC
Region
1
2a
2b
3
B
BODIPY 493/503
Hts
DAPI
10 µm
C
Nile Red
DAPI
10 µm
D
LipidTox
DAPI
10 µm
F
Day 1
Hts /LD/DAPI
Terminal Filament
5 µm
G
Day 3
5 µm
H
Day 8
5 µm
I
Number of Hts aggregate in terminal filamnet
Days
E
Lipid Droplet number in germarium
BODIPY
Nile Red
LipidTox
TF/CC Cells
Germ Cells
Follicle Cells
J
SH
TF
cap
EC
GSC

Fig. 1

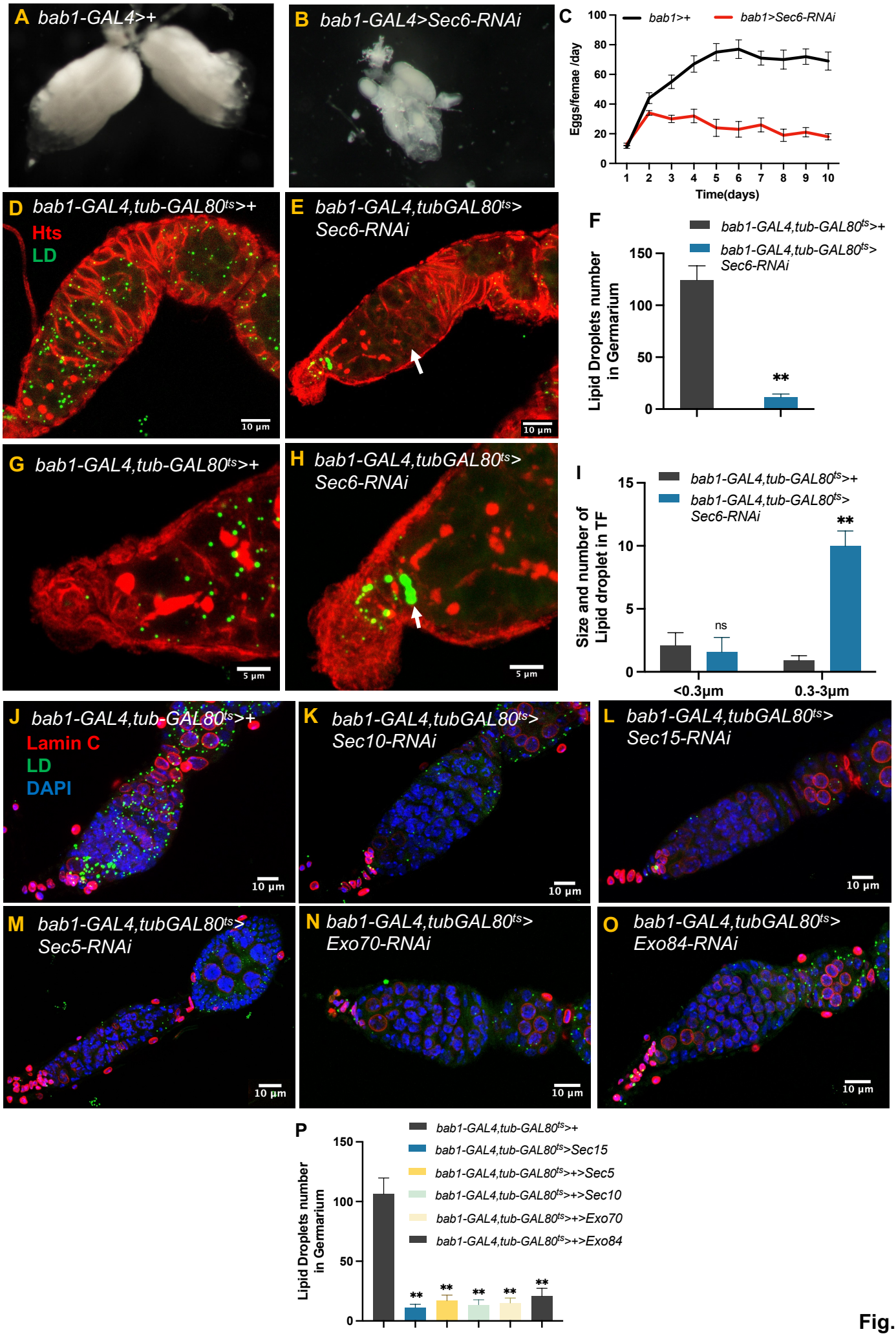
A bab1-GAL4>+
B bab1-GAL4>Sec6-RNAi
C
bab1>+
bab1>Sec6-RNAi
Eggs/femae /day
Time(days)
D bab1-GAL4,tub-GAL80ts>+
Hts
LD
10 μm
E bab1-GAL4,tubGAL80ts> Sec6-RNAi
10 μm
F
bab1-GAL4,tub-GAL80ts>+
bab1-GAL4,tub-GAL80ts> Sec6-RNAi
Lipid Droplets number in Germarium
**
G bab1-GAL4,tub-GAL80ts>+
5 μm
H bab1-GAL4,tubGAL80ts> Sec6-RNAi
5 μm
I
bab1-GAL4,tub-GAL80ts>+
bab1-GAL4,tub-GAL80ts> Sec6-RNAi
Size and number of Lipid droplet in TF
ns
**
<0.3μm
0.3-3μm
J bab1-GAL4,tub-GAL80ts>+
Lamin C
LD
DAPI
10 μm
K bab1-GAL4,tubGAL80ts> Sec10-RNAi
10 μm
L bab1-GAL4,tubGAL80ts> Sec15-RNAi
10 μm
M bab1-GAL4,tubGAL80ts> Sec5-RNAi
10 μm
N bab1-GAL4,tubGAL80ts> Exo70-RNAi
10 μm
O bab1-GAL4,tubGAL80ts> Exo84-RNAi
10 μm
P
bab1-GAL4,tub-GAL80ts>+
bab1-GAL4,tub-GAL80ts>Sec15
bab1-GAL4,tub-GAL80ts>+>Sec5
bab1-GAL4,tub-GAL80ts>+>Sec10
bab1-GAL4,tub-GAL80ts>+>Exo70
bab1-GAL4,tub-GAL80ts>+>Exo84
Lipid Droplets number in Germarium

Fig. 2

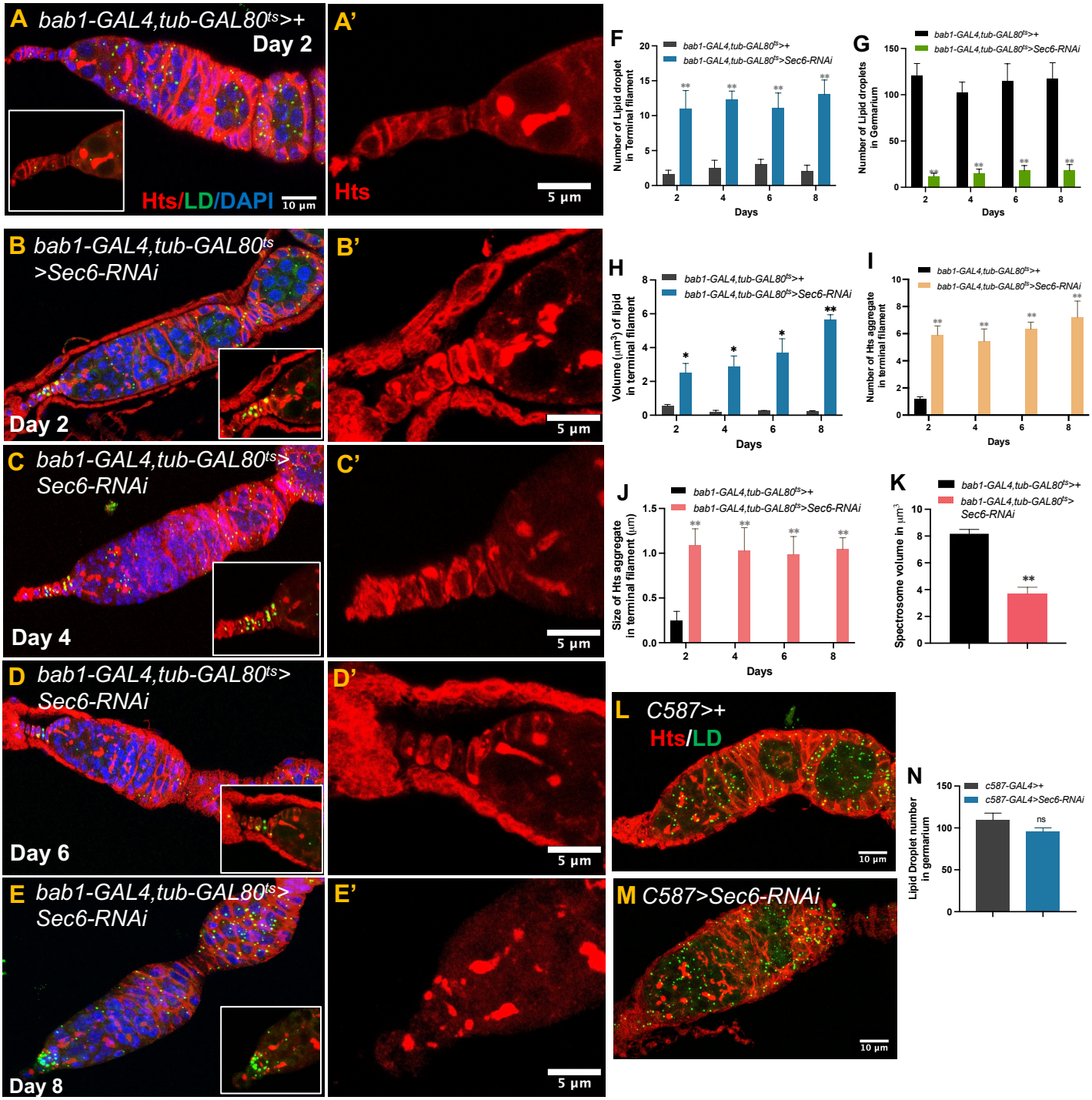
A bab1-GAL4,tub-GAL80ts>+
Day 2
Hts/LD/DAPI
10 µm
A'
Hts
5 µm
B bab1-GAL4,tub-GAL80ts >Sec6-RNAi
Day 2
B'
5 µm
C bab1-GAL4,tub-GAL80ts> Sec6-RNAi
Day 4
C'
5 µm
D bab1-GAL4,tub-GAL80ts> Sec6-RNAi
Day 6
D'
5 µm
E bab1-GAL4,tub-GAL80ts> Sec6-RNAi
Day 8
E'
5 µm
F
bab1-GAL4,tub-GAL80ts>+
bab1-GAL4,tub-GAL80ts>Sec6-RNAi
Number of Lipid droplet in Terminal filament
Days
G
bab1-GAL4,tub-GAL80ts>+
bab1-GAL4,tub-GAL80ts>Sec6-RNAi
Number of Lipid droplets in Germarium
Days
H
bab1-GAL4,tub-GAL80ts>+
bab1-GAL4,tub-GAL80ts>Sec6-RNAi
Volume (µm3) of lipid in terminal filament
Days
I
bab1-GAL4,tub-GAL80ts>+
bab1-GAL4,tub-GAL80ts>Sec6-RNAi
Number of Hts aggregate in terminal filament
Days
J
bab1-GAL4,tub-GAL80ts>+
bab1-GAL4,tub-GAL80ts>Sec6-RNAi
Size of Hts aggregate in terminal filament (µm)
Days
K
bab1-GAL4,tub-GAL80ts>+
bab1-GAL4,tub-GAL80ts> Sec6-RNAi
Spectrosome volume in µm3
L C587>+
Hts/LD
10 µm
M C587>Sec6-RNAi
10 µm
N
c587-GAL4>+
c587-GAL4>Sec6-RNAi
ns
Lipid Droplet number in germarium

Fig. 3

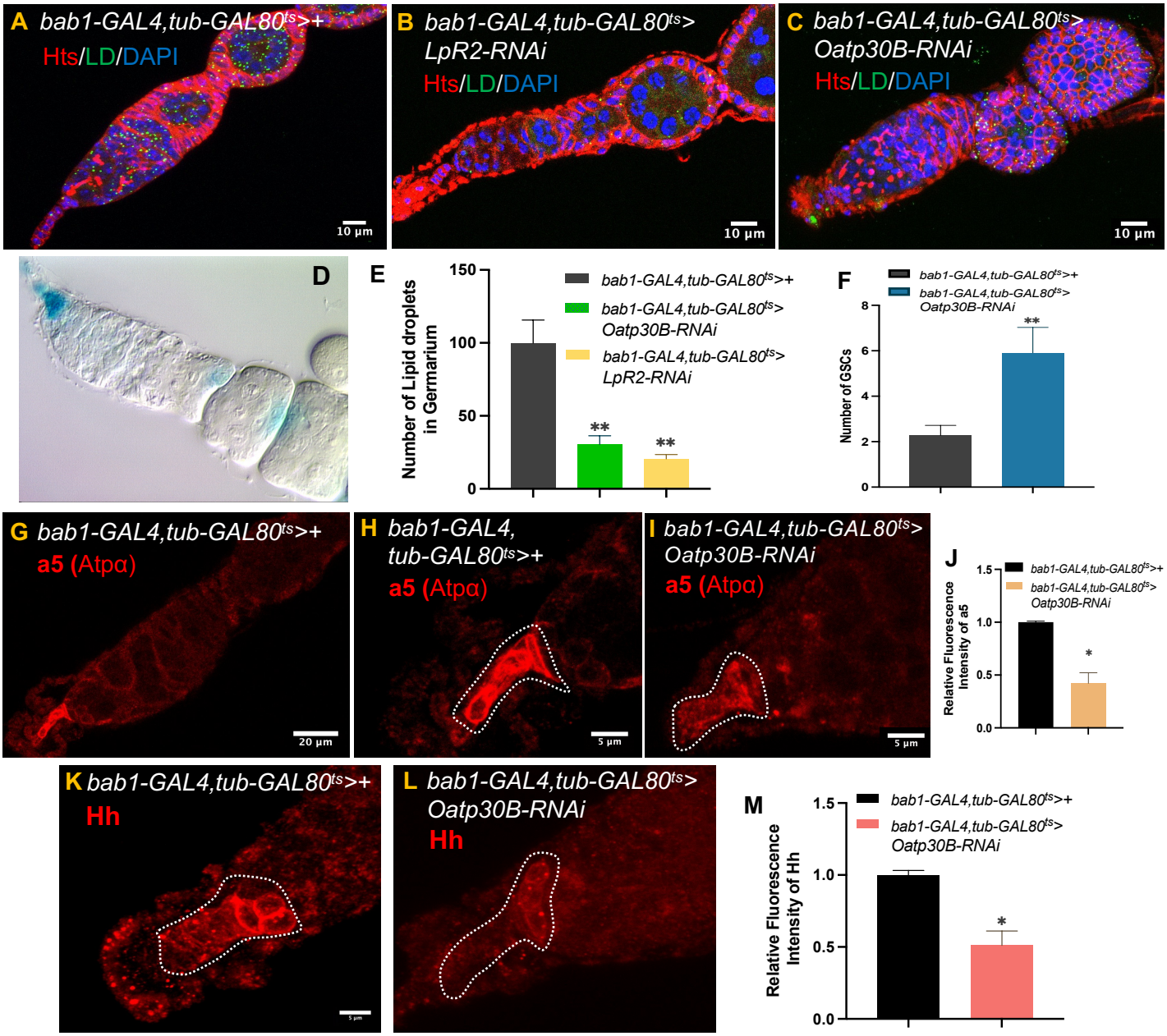
A bab1-GAL4,tub-GAL80ts>+
Hts/LD/DAPI
10 μm
B bab1-GAL4,tub-GAL80ts>
LpR2-RNAi
Hts/LD/DAPI
10 μm
C bab1-GAL4,tub-GAL80ts>
Oatp30B-RNAi
Hts/LD/DAPI
10 μm
D
E
Number of Lipid droplets in Germarium
150
100
50
0
**
**
bab1-GAL4,tub-GAL80ts>+
bab1-GAL4,tub-GAL80ts>
Oatp30B-RNAi
bab1-GAL4,tub-GAL80ts>
LpR2-RNAi
F
bab1-GAL4,tub-GAL80ts>+
bab1-GAL4,tub-GAL80ts>
Oatp30B-RNAi
Number of GSCs
8
6
4
2
0
**
G bab1-GAL4,tub-GAL80ts>+
a5 (Atpα)
20 μm
H bab1-GAL4,
tub-GAL80ts>+
a5 (Atpα)
5 μm
I bab1-GAL4,tub-GAL80ts>
Oatp30B-RNAi
a5 (Atpα)
5 μm
J
Relative Fluorescence Intensity of a5
1.5
1.0
0.5
0.0
*
bab1-GAL4,tub-GAL80ts>+
bab1-GAL4,tub-GAL80ts>
Oatp30B-RNAi
K bab1-GAL4,tub-GAL80ts>+
Hh
L bab1-GAL4,tub-GAL80ts>
Oatp30B-RNAi
Hh
M
Relative Fluorescence Intensity of Hh
1.5
1.0
0.5
0.0
*
bab1-GAL4,tub-GAL80ts>+
bab1-GAL4,tub-GAL80ts>
Oatp30B-RNAi

Fig. 4

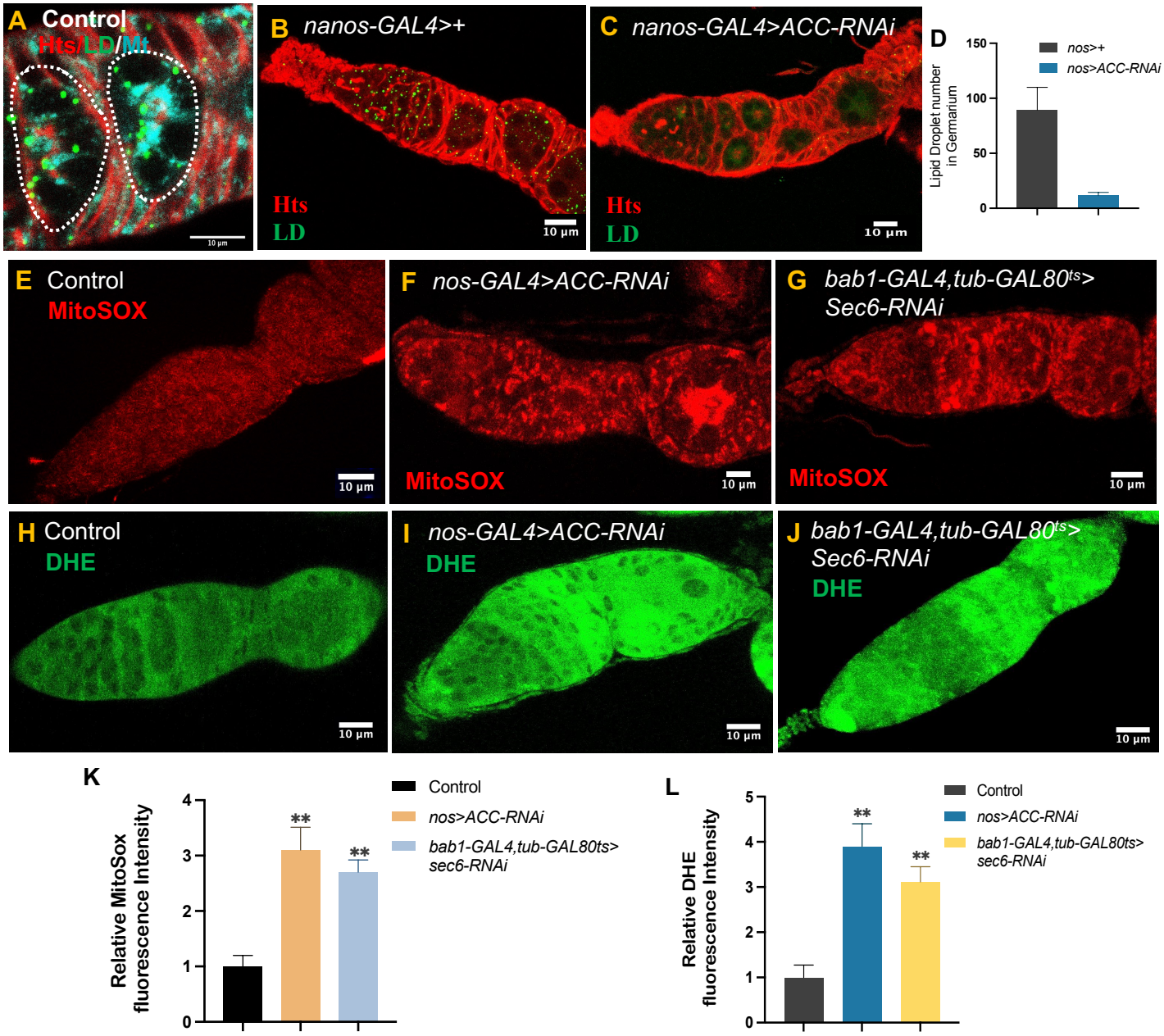
A Control
Hts/LD/Mt
10 μm
B nanos-GAL4>+
Hts
LD
10 μm
C nanos-GAL4>ACC-RNAi
Hts
LD
10 μm
D
Lipid Droplet number in Germarium
150
100
50
0
nos>+
nos>ACC-RNAi
E Control
MitoSOX
10 μm
F nos-GAL4>ACC-RNAi
MitoSOX
10 μm
G bab1-GAL4,tub-GAL80ts> Sec6-RNAi
MitoSOX
10 μm
H Control
DHE
10 μm
I nos-GAL4>ACC-RNAi
DHE
10 μm
J bab1-GAL4,tub-GAL80ts> Sec6-RNAi
DHE
10 μm
K
Relative MitoSox fluorescence Intensity
4
3
2
1
0
**
**
Control
nos>ACC-RNAi
bab1-GAL4,tub-GAL80ts> sec6-RNAi
L
Relative DHE fluorescence Intensity
5
4
3
2
1
0
**
**
Control
nos>ACC-RNAi
bab1-GAL4,tub-GAL80ts> sec6-RNAi

Fig.5

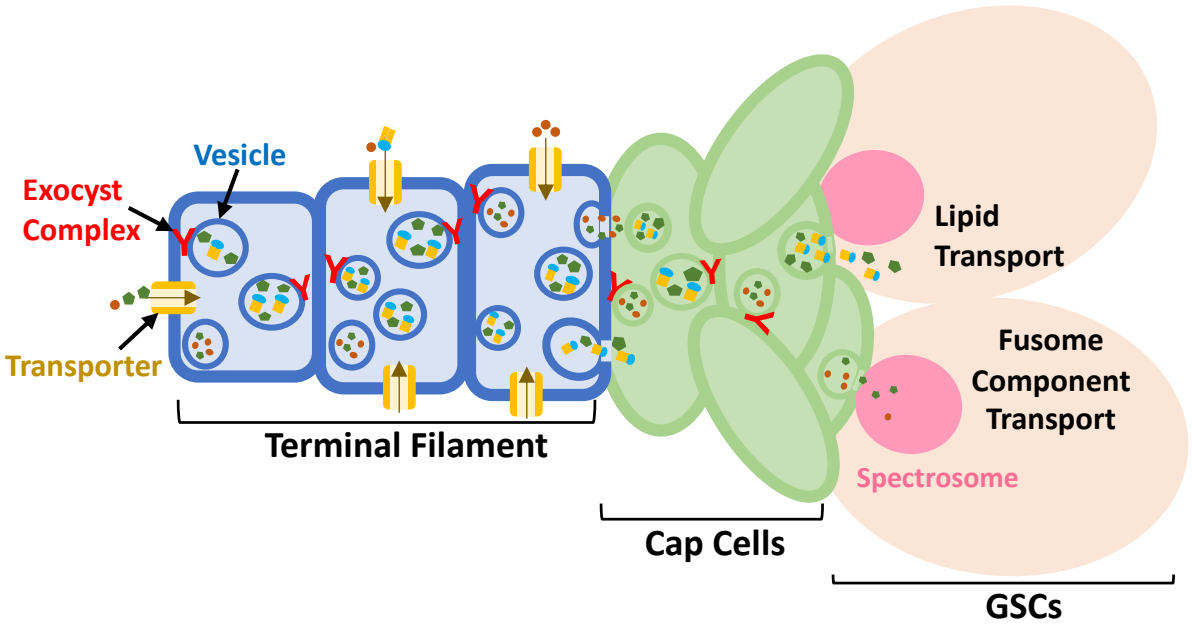
Vesicle
Exocyst
Complex
Transporter
Terminal Filament
Cap Cells
GSCs
Lipid
Transport
Fusome
Component
Transport
Spectrosome

Fig.6